PURE WATER ABSORPTION COEFFICIENT AROUND 400NM: LAB MEASURED VERSUS FIELD OBSERVED

Zhongping Lee, James E. Ivey, Kendall L. Carder, Robert G. Steward, and Jennifer S. Patch
Department of Marine Science, University of South Florida
140, 7th Ave. S., St. Petersburg, FL 33701
zplee@monty.marine.usf.edu
(727)553-3952

INTRODUCTION

From numerical studies [Gordon et al. 1988, Morel and Gentili 1993, Lee et al. 1999], it has been found that remote-sensing reflectance (or irradiance reflectance) of optically deep waters is a function of the ratio of the backscattering coefficient to the absorption coefficient (or the sum of absorption and backscattering coefficients), when there is no contribution from in-elastic scattering such as Raman scattering and fluorescence. To test how good those relationships hold in the field, extensive measurements along with modeling have been carried out [Carder and Steward 1985; Lee et al. 1994; Roesler and Perry 1995]. In general, it has been found that reflectance can be well explained (or modeled) using known absorption and backscattering coefficients of pure water, plus measured pigment absorption coefficients and bio-optical models regarding the absorption coefficient of gelbstoff and backscattering coefficient of particles [Sathyendranath et al. 1989, Lee et al. 1994]. Recently, we have made some measurements in very clear natural waters (Sargasso Sea), and found that there are some residual distinct mismatches near 400nm. This was also found for clear waters at other locations, such as the Pacific Ocean. Figure 1 shows examples of measured versus modeled $R_{rs}(\lambda)$ curves, where the values around 400nm are highlighted in the circles. Those residual differences cannot be resolved by adjusting the values of pigment absorption or gelbstoff absorption or the backscattering coefficients, unless we adjust at high resolution the spectral curvatures of those parameters.

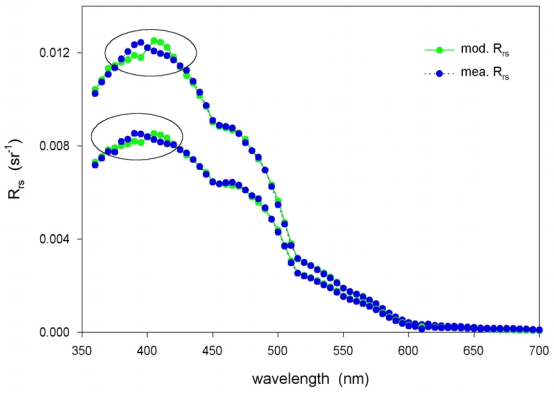

Figure 1. Measured versus modeled remote-sensing reflectance. Residual differences are highlighted in the circles.

Checking literature values of the absorption coefficients of pure waters, it is found that there are wide variations from measurement to measurement, especially at blue-green wavelengths [see Smith and Baker 1981, Buiteveld et al. 1994, Pope and Fry 1997 and Sogandares and Fry 1997]. For the consistent mismatch observed for various clear

waters, we suspect that one possible source may be the uncertainty of reported pure-water absorption values, since pure-water absorption plays a larger role for clear waters. For coastal waters, the mismatch was not observed.

To compare various pure-water absorption curves, we spectrally decomposed remote-sensing reflectance into spectra for absorption coefficients of pigments, water and gelbstoff and backscattering of particles, and assign the residual differences between measured and modeled R_{rs} to pure-water absorption coefficients. When comparing the derived a_w values with lab-measured values [Pope and Fry, 1997], it is found that 1) there is a substantial, high-resolution curvature difference around 400nm, and 2) the values could differ by as much as 20% from 380 to 420nm. The derived values, however, were more consistent with those from in-water diffuse attenuation measurements, but it is not clear yet what could be the possible reasons for the mismatch between the lab values and various field observations. Other than the wide variations among the reported pure-water absorption values, possible explanations are that absorption by gelbstoff and backscattering by particles may not be smooth functions of wavelength as are commonly used, and that bacteria may be perturbing factor near 400nm [Morel and Ahn, 1990].

DATA

Remote sensing reflectance curves of waters of the Sargasso Sea (1998, 1999) and of the Pacific Ocean (off Hawaii, 1997; off California, 1999) were measured. Pigment absorption coefficients of the waters of the Sargasso Sea were measured in May 1998 and May 1999. The downwelling diffuse attenuation coefficient (K_d) curves of Sargasso Sea waters were measured in May 1999. All measurement methods were based on the SeaWiFS protocols [Mueller and Austin, 1992].

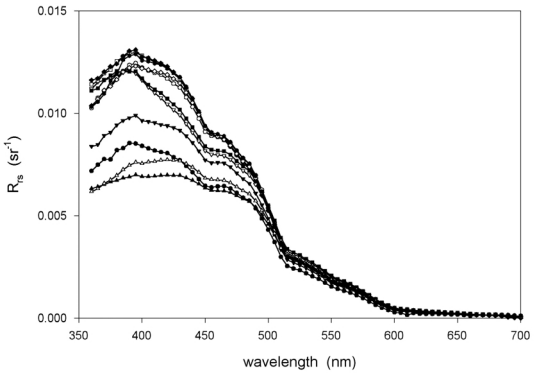

Figure 2. Measured remote-sensing reflectance of the Sargasso Sea.

Briefly, the method of Lee et al [1996] was used for the determination of R_{rs}, with downwelling irradiance and upwelling radiance measured using SPECTRIX, a spectroradiometer with 512 spectral bands covering a wavelength range from 350 to 900nm. Results matched those using Carder and Steward [1985] method for this study as the waters were very clear (chlorophyll concentration less than 0.1 mg/m^3 and the waters were far from coastal runoff) and solar zenith angles exceeded 30^o. Figure 2 shows some of the measured R_{rs} used in this study.

Pigment absorption coefficients, $a_\phi(\lambda)$, were determined from collected surface water samples as described in Kishino et al [1983] and Roesler et al. [1989], with the "β factor" of Carder et al. [1999]. From those measured $a_\phi(\lambda)$, 440nm normalization of the curves ($a_\phi^+(\lambda) = a_\phi(\lambda)/a_\phi(440)$) was performed, and very limited variations among those

curves were observed. Figure 3 shows the results, where the solid line is the average and was used in the following spectral decomposition. This averaged curvature is consistent with those measured by Allali et al. [1997] and Bricaud et al. [1998].

Downwelling diffuse attenuation coefficients were determined as in Smith and Baker [1981] by performing regression of the logarithm of the downwelling irradiance versus depth for the upper water column. Downwelling irradiance at depth was measured using a slow-dropping package well away from the ship. The package uses a SPECTRIX observing diffuse light through a Tyler and Smith [1970] diffuser to measure downwelling irradiance. Figure 4 shows the K_d curves used in this study. Note the similarity in curve shapes, but wide variation in values, as the waters were similar in constituents but the measurements were made at different solar zenith angles.

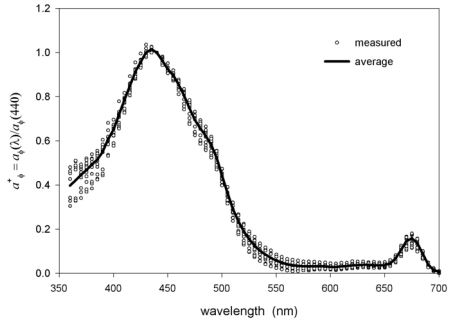

Figure 3. Measured, 440nm-normalized, pigment absorption coefficient of clear waters.

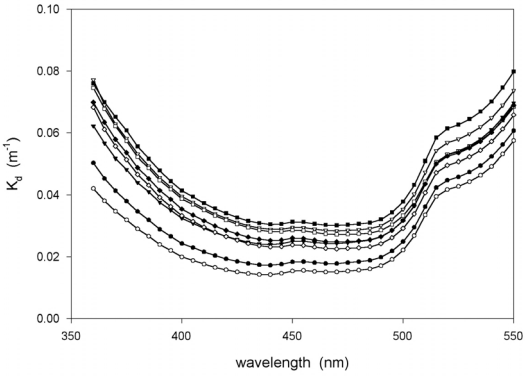

Figure 4. Measured downwelling diffuse attenuation coefficient.

a_w DETERMINATION

From R_{rs}

For optically deep, open ocean waters there is [Gordon et al. 1988]

$$R_{rs} \approx G(0.0949 + 0.0794u)\,u\,, \qquad (\mathbf{1})$$

where G is the air-sea interface factor, which approximates 0.54 [Mobley 1994] for open ocean waters.

In Eq.1,

$$u = b_b/(a+b_b), \qquad (\mathbf{2})$$

and,

$$b_b = b_{bw} + b_{bp}, \qquad (\mathbf{3})$$

$$a = a_w + a_\phi + a_g. \qquad (\mathbf{4})$$

b_{bw} and a_w are the backscattering coefficient and absorption coefficient of water molecules. Their values are taken from Morel [1974] and Pope and Fry [1997], respectively. b_{bp}, a_ϕ and a_g are the backscattering coefficient of particles, and absorption coefficients of pigments and gelbstoff, respectively. They are modeled as follows:
$b_{bp}(\lambda)$ is expressed as

$$b_{bp}(\lambda) = X\left(\frac{400}{\lambda}\right)^{Y}, \tag{5}$$

where $X = b_{bp}(400)$. Y is the spectral shape parameter of particle backscattering. A value of 2.5 is used, consistent with open ocean waters [Sathyendranath et al 1989, Lee et al. 1999].

To overcome the noise in measured $a_\phi(\lambda)$, $a_\phi(\lambda)$ is simulated by a single-parameter model, using the average of the measured, 400nm-normalized, pigment absorption curvature of clear waters:

$$a_\phi(\lambda) = P\ a_\phi^+(\lambda), \tag{6}$$

with $P = a_\phi(440)$.

$a_g(\lambda)$ is expressed as [Bricaud et al. 1981, Roesler et al. 1989, Carder et al. 1991]

$$a_g(\lambda) = G\, e^{-S(\lambda-440)}, \tag{7}$$

with $G = a_g(440)$. S is the spectral slope, and a value of 0.015nm^{-1} is used as a representative average.

Inverting measured $R_{rs}(\lambda)$, $a_w(\lambda)$ is derived as follows: Eq. 1 is rewritten as

$$R_{rs} \approx A_0 u + A_1 u^2, \tag{8}$$

then,

$$u = \frac{-A_0 + \sqrt{A_0^2 + 4A_1 R_{rs}}}{2A_1} \tag{9}$$

$$\downarrow$$

$$a = \frac{b_b - u b_b}{u} \tag{10}$$

$$\downarrow$$

$$a_w(\lambda) = a(\lambda) - P\, a_\phi^+(\lambda) - G\, e^{-S(\lambda-440)} \tag{11}$$

Using an optimization process [Lee et al. 1996, 1999] to force derived $a_w(\lambda)$ curves to match the values of Pope and Fry [1997] at blue-green wavelengths, values for P, G and X were derived, and a_w values were then determined. Essentially, the residual differences between measured and modeled R_{rs} were assigned to the values of a_w.

From K_d

From Gordon [1989], K_d can be expressed as

$$K_d(\lambda) \approx D\left(a(\lambda) + b_b(\lambda)\right) \tag{12}$$

where D is the averaged distribution function for the upper water column [Gordon 1989]. Combining Eqs.5 - 7,

$$a_w(\lambda) \approx K_d(\lambda)/D - P\,a_\phi^+(\lambda) - G\,e^{-S(\lambda-440)} - b_{bw}(\lambda) - X\left(\frac{400}{\lambda}\right)^{2.5} \quad \textbf{(13)}$$

Forcing by optimization the derived $a_w(\lambda)$ to match the values of Pope and Fry [1997] at blue-green wavelengths, a set of values for *D, P, G* and *X* were derived, as well as the values for $a_w(\lambda)$ for that region. Note that due to the similarity in spectral curvatures between $a_g(\lambda)$ and $b_{bp}(\lambda)$, derived *X* values are only approximate.

RESULTS AND DISCUSSION

Figure 5 shows the a_w values derived from R_{rs}, with the solid line as the average of 30 samples. The biggest percentage variation is 7.0% (at 405 nm), with an average variation of 3.8% for the 360 to 500nm region. This suggests R_{rs}→a_w values are consistent from sample to sample, although each one has slightly different constituents. Inversions using different values of *Y* and *S* were studied and no significant difference was found in derived R_{rs}→a_w values, suggesting some compensation occurs between values of *P* and *G* for different values of *Y* and *S*.

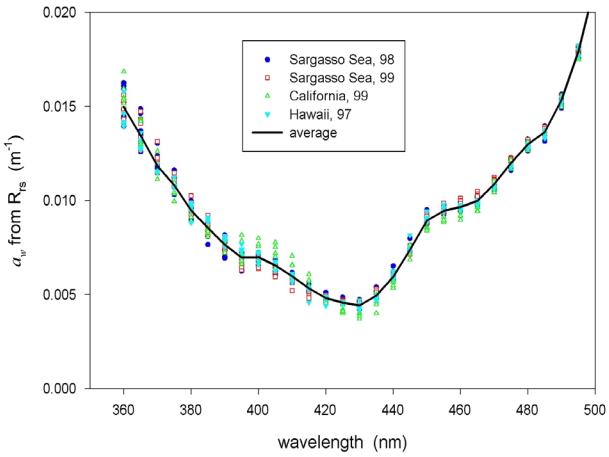

Figure 5. Derived $a_w(\lambda)$ from R_{rs}.

Figure 6 shows the $a_w(\lambda)$ values derived from $K_d(\lambda)$, with the solid line as the average of 7 samples. The biggest percentage variation is 5.2% (at 360nm), with an average variation of 1.7% for the 360 to 500nm region. This suggests that K_d→a_w values are consistent with each other.

Figure 7 presents field-observed and lab-measured a_w values together. Since the values of Pope and Fry [1997] were used as the reference curve in the process of deriving a_w from field data, we see

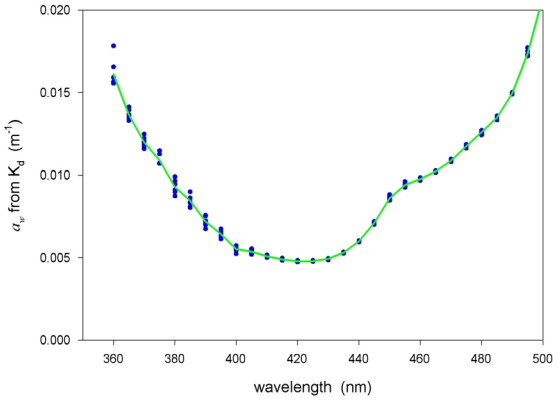

Figure 6. Derived $a_w(\lambda)$ from K_d.

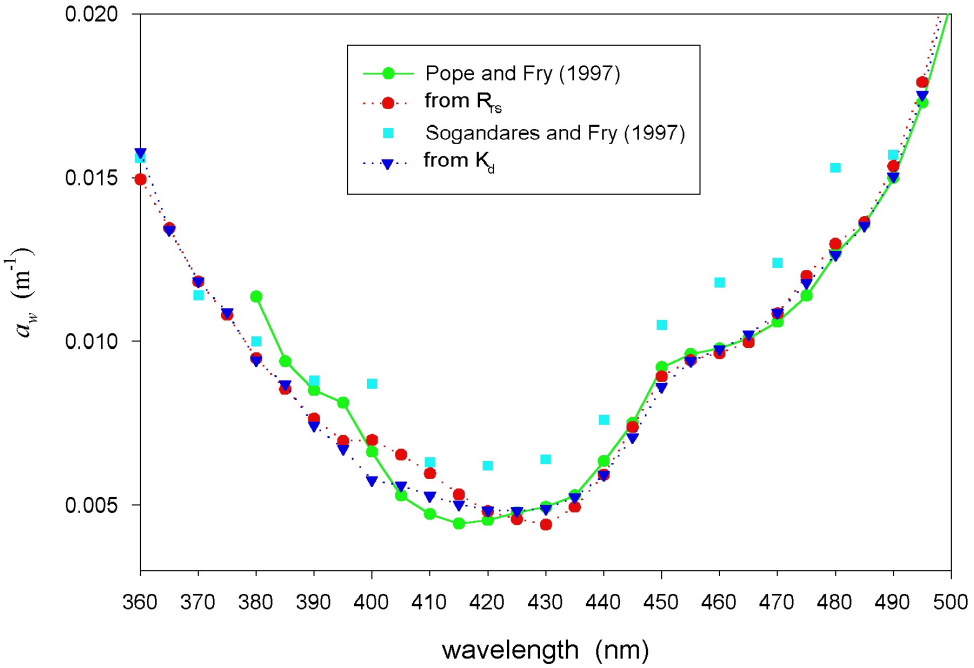

Figure 7. Comparing field observed a_w values to lab measured a_w values for the blue-green wavelengths.

both R_{rs}→a_w and K_d→a_w values match the Pope and Fry [1997] values very well from 420 to 500nm. R_{rs}→a_w and

K_d→a_w values also match Sogandares and Fry [1997] values in the 360 - 380nm region, as those values were used as reference for the shorter wavelength range, where Pope and Fry [1997] did not provide values. It is found that all derived values fall in the accuracy range (~10%) of Pope and Fry [1997], and more importantly the derived R_{rs}→a_w values work well in modeling measured $R_{rs}(\lambda)$ for both clear and coastal waters.

R_{rs}→a_w values generally match K_d→a_w values well in the 360 - 500nm region, suggesting both measurements and approaches are consistent. The missing bump in K_d→a_w at 400nm may be due to the limited attenuation lengths in the measurement of downwelling irradiance, as there were curvature changes in measured R_{rs} at 400nm (Figs. 1 and 2), but no such changes in measured K_d at 400nm. The missing bump may also come from errors in modeling b_{bp}, as b_{bp} has much greater influence on R_{rs} than on K_d. Morel and Ahn [1990] show that bacteria provide perturbations in rather smooth backscattering and absorption curves near 400nm, and that GF/F filters could undersample them for $a_\phi(\lambda)$ determination.

R_{rs}→a_w does not match the values of Pope and Fry [1997] from 380 to 415nm, with the biggest difference (23%) appearing at 410nm. R_{rs}→a_w shows a minimum at 430nm, instead of the minimum at 415nm of Pope and Fry [1997].

It is not clear what may be the reasons for the a_w mismatch here, although we realize that both methods are not perfect for accurate determination of absorption coefficient of pure waters. We notice that the counts of upwelling radiance from SPECTRIX in the 400nm region were not small (> 100 counts above dark counts) and we did average many (>5) water scans to increase signal-to-noise ratio in those measurements. Spectral calibration for SPECTRIX was performed before and after each cruise, and the precision is about 1 nm.

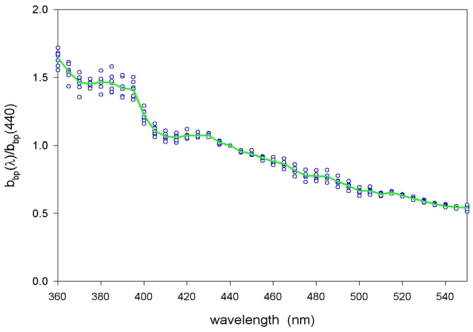

Figure 8. Derived $b_{bp}^{+}(\lambda)$, line for average.

Other possible sources of error include effects from CDOM fluorescence and Raman scattering. It has been found that CDOM fluorescence is broad-band (>50nm in width) effect and peaked in the longer wavelengths (~500nm) [Hawes 1992, Lee et al. 1994], therefore we may exclude CDOM fluorescence as a possible cause. We did some preliminary tests regarding effects of Raman scattering on the $R_{rs} \rightarrow a_w$ determination, and did not found a significant impact on the derived $R_{rs} \rightarrow a_w$ values.

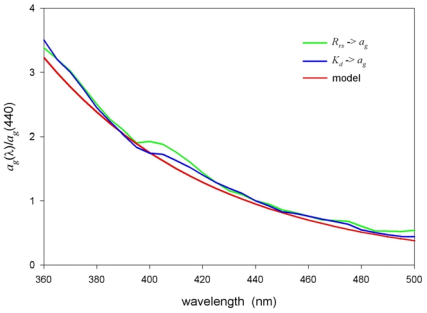

Figure 9. $a_g^{+}(\lambda)$ comparison.

More likely sources of error may come from the empirical models of $a_g(\lambda)$ and $b_{bp}(\lambda)$. In reality those models are not perfect. As a result, we have assigned the residual difference to the curvatures of $b_{bp}(\lambda)$ or $a_g(\lambda)$. Figure 8 and Figure 9 show the results. Clearly, the derived $b_{bp}(\lambda)$ curvature is somewhat "strange", but is not inconsistent with backscattering perturbations proposed by Carder et al. [1986] and those from bacteria measured by Morel and Ahn [1990]. The derived $a_g(\lambda)$ curvatures from both R_{rs} and K_d, however, are similar to those of Bricaud et al. [1981] in the 400nm region, though they are spectrally dissimilar in terms of spectral width.

If this is the answer regarding the a_w mismatch here, we may have to be more careful in modeling $a_g(\lambda)$ if we want to fit the measured $R_{rs}(\lambda)$ more tightly, or improve the accuracy in retrieving pigment concentration using analytical/semi-analytical algorithms [Carder et al. 1999, Garver and Siegel 1997], at present it is quite difficult to measure ag(λ) at visible wavelengths in clear waters, and improved methods are meeded.

ACKNOWLEDGEMENT

Financial support was provided by the following contracts and grants: NASA through NAS5-97137, NAS5-31716 and NAG5-3446; the Office of Naval Research

through N00014-96-I-5013, and N00014-97-0006; and the NOAA Coastal Ocean Program R/NCOP-5.

REFERENCES

Allali, K., A. Bricaud, and H. Claustre, Spatial variations in the chlorophyll-specific absorption coefficients of phytoplankton and photosynthetically active pigments in the equatorial Pacific, *J. Geophys. Res. 102*, 12,413-12,423, 1997.

Bricaud, A., A. Morel, M. Babin, K. Allali, and H. Claustre, Variations of light absorption by suspended particles with chlorophyll a concentration in oceanic (case 1) waters: Analysis and implications for bio-optical models, *J. Geophys. Res. 103*, 31,033-31,044, 1998.

Bricaud, A., A. Morel, and L. Prieur, Absorption by dissolved organic matter of the sea (yellow substance) in the UV and visible domains, *Limnol. Oceanogr. 26*, 43-53, 1981.

Buiteveld, H., J. H. M. Hakvoort and M. Donze, The optical properties of pure water, *Ocean Optics XII*, 174-183, 1994.

Carder, K. L., and R. G. Steward, A remote-sensing reflectance model of a red tide dinoflagellate off West Florida, *Limnol. Oceanogr. 30*, 286-98, 1985.

Carder, K. L., R. G. Steward, J. H. Paul, G. A. Vargo, Relationship between chlorophyll and ocean color constituents as they affect remote-sensing reflectance models, *Limnol. Oceanogr. 31*, 403-413, 1986.

Carder, K. L., S. K. Hawes, K. A. Baker, R. C. Smith, R. G. Steward, and B. G. Mitchell, Reflectance model for quantifying chlorophyll a in the presence of productivity degradation products, *J. Geophys. Res. 96*, 20599-20611, 1991.

Carder, K. L., F. R. Chen, Z. P. Lee, S. K. Hawes, D. Kamykowski, Semianalytic moderate-resolution imaging spectrometer algorithms for chlorophyll a and absorption with bio-optical domains based on nitrate-depletion temperatures, *J. Geophys. Res. 104*, 5403-5421, 1999.

S. A. Garver and D. Siegel, Inherent optical property inversion of oceanic color spectra and its biogeochemical interpretation 1. Time series from the Sargasso Sea, *J. Geophys. Res. 102*, 18,607-18,625, 1997.

Gordon, H. R., O. B. Brown, R. H. Evans, J. W. Brown, R. C. Smith, K. S. Baker, and D. K. Clark, A semianalytic radiance model of ocean color, *J. Geophys. Res. 93*, 10,909-10,924, 1988.

Gordon, H. R., Can the Lambert-Beer law be applied to the diffuse attenuation coefficient of ocean water? *Limnol. Oceanogr., 34*, 1389-409, 1989.

Hawes, S. K., K. L. Carder, and G. R. Harvey, Quantum fluorescence efficiencies of marine humic and fulvic acids: effects on ocean color fluorometric detection, Ocean Optics XI, G. D. Gilbert ed., SPIE 1750, 212-223, 1992.

Kishino, M., M. Takahashi, N. Okami, and S. Ichimura, Estimation of the spectral absorption coefficients of phytoplankton in a thermally stratified sea, *Bull. Mar. Sci. 37*, 634-42, 1985.

Lee, Z. P., K. L. Carder, S. K. Hawes, R. G. Steward, T. G. Peacock, and C. O. Davis, A model for interpretation of hyperspectral remote sensing reflectance, *Appl. Opt., 33*, 5721-5732, 1994.

Lee, Z. P., K. L. Carder, R. G. Steward, T. G. Peacock, C. O. Davis, and J. L. Mueller, Remote-sensing reflectance and inherent optical properties of oceanic waters derived from above-water measurements, *Ocean Optics XIII*, SPIE Vol. *2963*, 160-166, 1996.

Lee, Z. P., K. L. Carder, C. Mobley, R. G. Steward, and J. S. Patch, Hyperspectral remote sensing for shallow waters: 2. Deriving Bottom Depths and Water Properties by Optimization, *Appl. Opt.*, *38*, 3831-3843, 1999.

Mobley, C.D. 1994. *Light and Water: radiative transfer in natural waters*. Academic Press. New York.

Morel, A., Optical properties of pure water and pure sea water, In *Optical aspects of oceanography,* ed. N. G. Jerlov and E. S. Nielsen, 1-24. New York: Academic. 1974.

Morel, A. and Y. H. Ahn, Optical efficiency factors of free-living marine bacteria: Influence of bacterioplankton upon the optical properties and particulate organic carbon in oceanic waters, *J. of Marine Research, 48*, 145-175, 1990.

Morel, A. and B. Gentili, Diffuse reflectance of oceanic waters (2): Bi-directional aspects, *Appl. Opt. 32*, 6864-879, 1993.

Mueller, J. L. and R. W. Austin, Ocean optics protocols for SeaWiFS validation. *NASA Technical Memorandum 104566, Vol. 5*, S. B. Hooker and E. R. Firestone, eds., NASA Goddard Space Flight Center, Greenbelt, MD, 1992.

Pope, R., and E. Fry, Absorption spectrum (380 - 700nm) of pure waters: II. Integrating cavity measurements, *Appl. Opt. 36*, 8710-8723, 1997.

Roesler, C. S., M. J. Perry, and K. L. Carder, Modeling in situ phytoplankton absorption from total absorption spectra in productive inland marine waters, *Limnol. Oceanogr. 34*, 1510-523, 1989.

Roesler, C. S. and M. J. Perry, In situ phytoplankton absorption, fluorescence emission, and particulate backscattering spectra determined from reflectance, *J. Geophys. Res., 100*, 13,279-294, 1995.

Sogandares, F. M. and E. S. Fry, Absorption spectrum (340 - 640 nm) of pure water. 1. Photothermal measurements, Appl. Opt. 36, 8699 - 8709, 1997.

Sathyendranath, S., L. Prieur, and A. Morel, A three-component model of ocean colour and its application to remote sensing of phytoplankton pigments in coastal waters. *Int. J. Remote Sensing 10* ,1373-394, 1989.

Smith, R. C., and K. S. Baker, Optical properties of the clearest natural waters, *Appl. Opt., 20*, 177-84, 1981.

Tyler, J. E. and R. C. Smith, Measurement of spectral irradiance underwater. New York: Gordon and Breach, 1970.